

Modern stellar dynamics, lecture 3: gravitational potential

Eugene Vasiliev

Institute of Astronomy, Cambridge

Part III / MAst course, Winter 2022

Gravitational potential

$$\nabla^2 \Phi = 4\pi G \rho \quad (\text{in Newtonian gravity})$$

$$G \approx 0.0043 \frac{\text{pc (km/s)}^2}{M_\odot}.$$

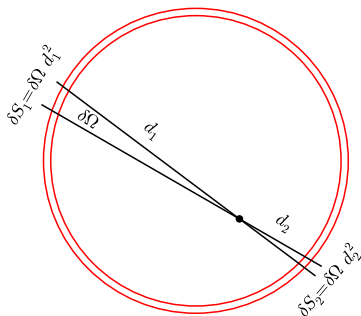
In galactic dynamics:

- ▶ neglect relativity;
- ▶ neglect cosmological expansion;
- ▶ [usually] Φ is negative and tends to zero at infinity.

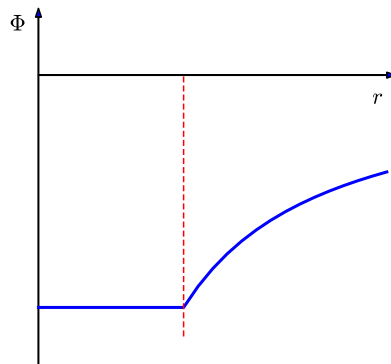
Formal solution of the Poisson equation (*not* a practically useful expression):

$$\Phi(\mathbf{x}) = - \iiint d^3x' \frac{G \rho(\mathbf{x}')}{|\mathbf{x} - \mathbf{x}'|}$$

Gravitational potential of spherical systems



Newton's 1st theorem:
a body inside a spherical shell with uniform density experiences no net gravitational force.



Newton's 2nd theorem:
the force outside a spherical shell of total mass M is the same as from a point mass.

Both results directly follow from Gauss's divergence theorem.

Gravitational potential of spherical systems

density profile $\rho(r) = \frac{1}{4\pi G} \nabla^2 \Phi = \frac{1}{4\pi G} \frac{1}{r^2} \frac{d}{dr} \left(r^2 \frac{d\Phi}{dr} \right)$

\Downarrow

enclosed mass $M(< r) \equiv \int_0^r ds \, 4\pi s^2 \rho(s)$

radial force ~~force~~
acceleration $F_r(r) \equiv -\frac{d\Phi(r)}{dr} = -\frac{G M(< r)}{r^2}$

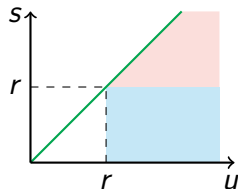
circular velocity $v_{\text{circ}}(r) \equiv \sqrt{r \frac{d\Phi}{dr}}$

\Downarrow

potential $\Phi(r) = \int_r^\infty du \, F_r(u) = -4\pi G \int_r^\infty du \int_0^u ds \, \frac{s^2 \rho(s)}{u^2}$

$$= -4\pi G \int_0^\infty ds \, s^2 \rho(s) \int_{\max(r,s)}^\infty du \, \frac{1}{u^2}$$

$$= -4\pi G \left[\frac{1}{r} \int_0^r ds \, s^2 \rho(s) + \int_r^\infty ds \, s \rho(s) \right]$$



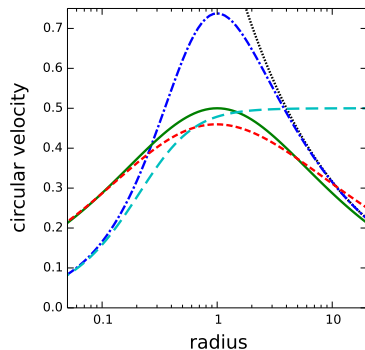
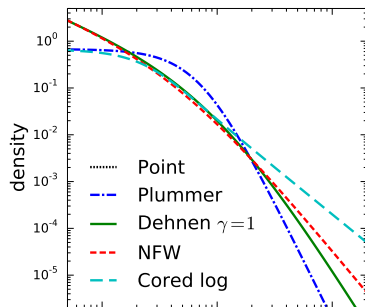
interior shells

exterior shells

Examples of spherical potentials

1. Power law: $\rho(r) = \rho_0 (r/a)^{-\gamma} \implies M(r) = \frac{4\pi \rho_0 a^3}{3-\gamma} (r/a)^{3-\gamma}$,
$$\Phi(r) = \begin{cases} \frac{4\pi G \rho_0 a^2}{(3-\gamma)(2-\gamma)} (r/a)^{2-\gamma} & \text{if } \gamma \neq 2, \\ 4\pi G \rho_0 a^2 \ln(r/a) & \text{if } \gamma = 2. \end{cases}$$
2. Plummer model: $\Phi(r) = -\frac{GM}{\sqrt{r^2+a^2}}.$
3. Dehnen model: $\Phi(r) = -\frac{GM}{(2-\gamma)a} \left[1 - \left(\frac{r}{r+a} \right)^{2-\gamma} \right] \quad (\gamma < 2).$
4. NFW model: $\Phi(r) = -\frac{GM}{r} \ln \left[1 + \frac{r}{a} \right].$
5. Cored logarithmic: $\Phi(r) = v_{\text{circ}}^2 \ln(1 + r/a).$

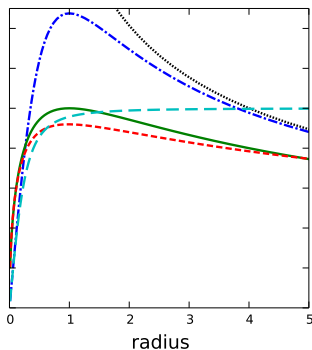
Circular-velocity curves



for a spherical potential,

$$v_{\text{circ}}(r) \equiv \sqrt{r \frac{d\Phi}{dr}} = \sqrt{\frac{G M(< r)}{r}}.$$

Cored density profiles have $v_{\text{circ}} \propto r$ at small r ;
 logarithmic potential has a “flat **rotation curve**”
 $v_{\text{circ}} \rightarrow v_0$ at large r .

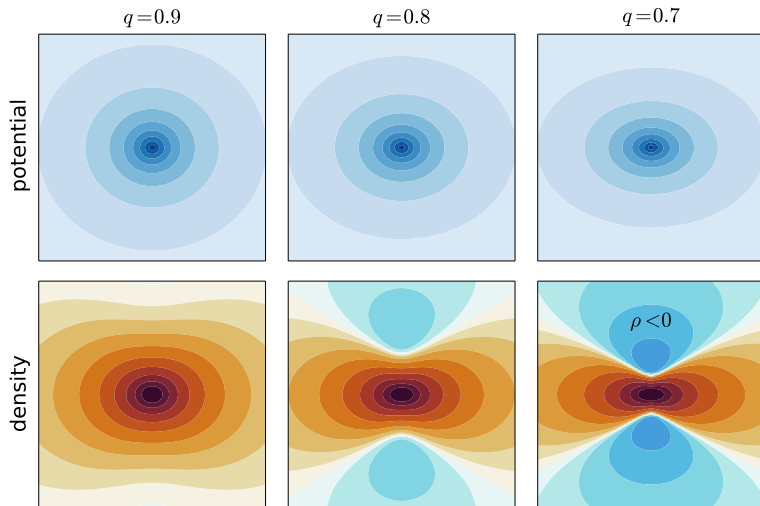


term strictly applicable only to gas motion, which is indeed nearly circular; mean stellar rotation velocity may be significantly smaller than v_{circ} , so to avoid confusion, it's better to call this “circular-velocity curve”

Ellipsoidal potentials

Substitute the ellipsoidal radius $m \equiv \sqrt{x^2 + (y/p)^2 + (z/q)^2}$ into expressions for spherical potential models (e.g., Dehnen $\gamma = 1$ in this example).

The result is disappointing – density becomes negative at large r .

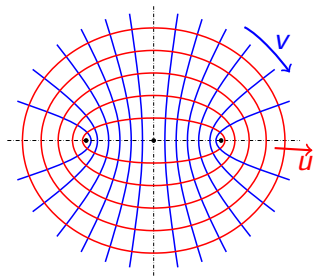


Potential of ellipsoidal density profiles

Substitute the ellipsoidal radius $m \equiv \sqrt{x^2 + (y/p)^2 + (z/q)^2}$ into expressions for spherical *density* profiles and compute the potential.

Introduce a coordinate system based on *confocal* ellipses and hyperbolae:

not concentric (similar)



2d elliptic coordinates

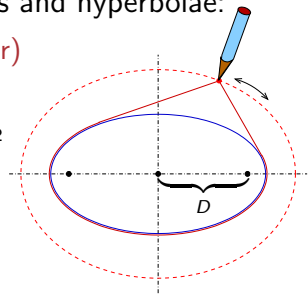
limiting cases:

$D \rightarrow 0$ – spherical: $u \rightsquigarrow r, v \rightsquigarrow \theta$

$D \rightarrow \infty$ – cylindrical: $u \rightsquigarrow z, v \rightsquigarrow R$

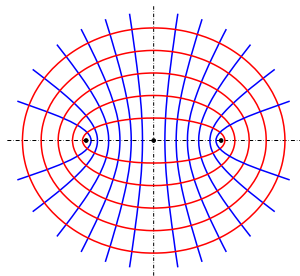
$$\begin{aligned}\text{ellipses: } & \frac{R^2}{\cosh^2 u} + \frac{z^2}{\sinh^2 u} = D^2 \\ \text{hyperbolae: } & \frac{R^2}{\sin^2 v} - \frac{z^2}{\cos^2 v} = D^2\end{aligned}$$

$$\begin{aligned}R &= D \cosh u \sin v, \\ z &= D \sinh u \cos v, \\ u &\geq 0, \quad 0 \leq v \leq \pi\end{aligned}$$

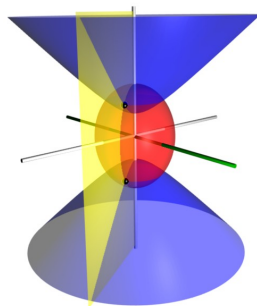


how to draw confocal ellipses
[Graves 1850, bishop of Limerick]

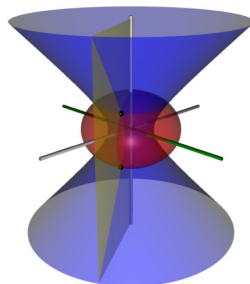
Ellipsoidal coordinates



2d elliptic coordinates

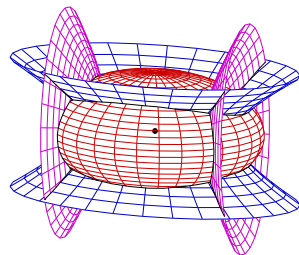


prolate spheroidal

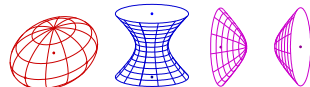


oblate spheroidal

[spheroid is an ellipsoid
with two equal axes]



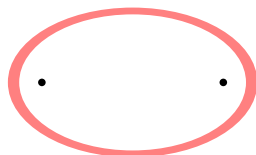
triaxial ellipsoidal



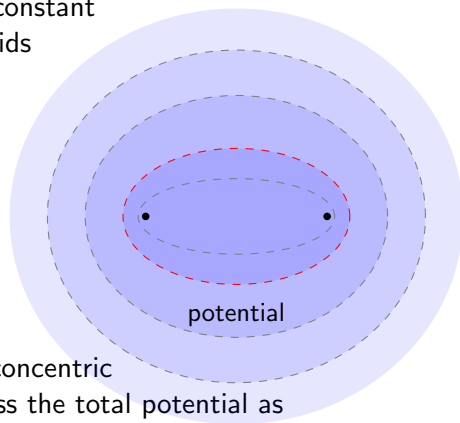
[from Wikipedia]

Potential of ellipsoidal density profiles

It turns out that the potential created by a thin uniform-density homoeoid (region between two *similar* ellipsoidal shells) is constant inside the shell, and stratified on *confocal* ellipsoids outside the shell (i.e. gets rounder with radius).



density



potential

By breaking down a density profile stratified on concentric (similar) ellipsoids into thin shells, one can express the total potential as

$$\Phi(\mathbf{x}) = -2\pi G p q \int_0^\infty d\tau \frac{\xi(m(\tau))}{\sqrt{(\tau+1)(\tau+p^2)(\tau+q^2)}},$$

$$\xi(m) \equiv \int_m^\infty dm m \rho(m), \quad m^2(\tau) \equiv \frac{x^2}{\tau+1} + \frac{y^2}{\tau+p^2} + \frac{z^2}{\tau+q^2}.$$

(typically
evaluated
numerically)

Stäckel potentials

A general triaxial ellipsoidal coordinate system λ, μ, ν is defined by two focal distances; coordinate lines of constant λ are confocal ellipses, constant μ – one-sheet hyperboloids, and constant ν – two-sheet hyperboloids.

A potential in a triaxial ellipsoidal coordinate system has a Stäckel form if

$$\Phi(\lambda, \mu, \nu) = \frac{f_\lambda(\lambda)}{(\lambda - \mu)(\nu - \lambda)} + \frac{f_\mu(\mu)}{(\mu - \nu)(\lambda - \mu)} + \frac{f_\nu(\nu)}{(\nu - \lambda)(\mu - \nu)}.$$

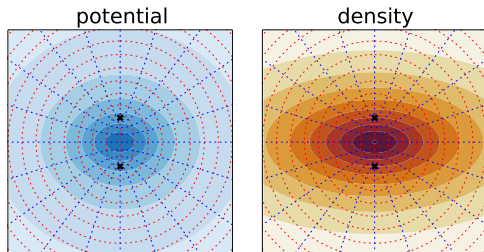
These potentials are important as the most general case in which the equations of motion are separable, as we will discuss in the next lecture.

A particularly “simple” example is the Perfect Ellipsoid model [de Zeeuw 1985]:

$$\rho(\mathbf{x}) = \frac{M a}{\pi^2 p q} \frac{1}{[a^2 + x^2 + (y/p)^2 + (z/q)^2]^2};$$

(Φ is expressed in terms of elliptic integrals).

Note that an *oblate* Perfect Ellipsoid density corresponds to a *prolate* spheroidal coordinate system for the potential!



Multipole expansion

Laplacian in spherical coordinates r, θ, ϕ :

$$\nabla^2 \Phi = \frac{1}{r^2} \frac{\partial}{\partial r} \left(r^2 \frac{\partial \Phi}{\partial r} \right) + \frac{1}{r^2 \sin \theta} \frac{\partial}{\partial \theta} \left(\sin \theta \frac{\partial \Phi}{\partial \theta} \right) + \frac{1}{r^2 \sin^2 \theta} \frac{\partial^2 \Phi}{\partial \phi^2}.$$

Consider first the angular part of the Laplacian – its eigenfunctions are [real-valued] spherical harmonics satisfying $\nabla^2 Y_\ell^m(\theta, \phi) = -\frac{\ell(\ell+1)}{r^2} Y_\ell^m(\theta, \phi)$:

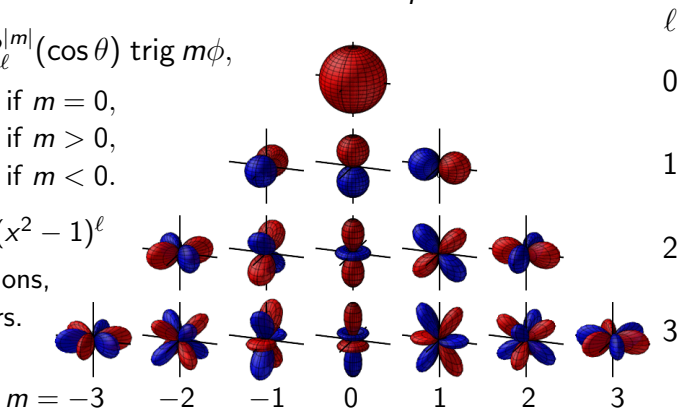
$$Y_\ell^m(\theta, \phi) \equiv \sqrt{\frac{2\ell+1}{4\pi} \frac{(\ell-|m|)!}{(\ell+|m|)!}} P_\ell^{|m|}(\cos \theta) \text{ trig } m\phi,$$

$$\text{trig } m\phi \equiv \begin{cases} 1 & \text{if } m = 0, \\ \sqrt{2} \cos m\phi & \text{if } m > 0, \\ \sqrt{2} \sin |m|\phi & \text{if } m < 0. \end{cases}$$

$$P_\ell^m(x) \equiv \frac{(-1)^m (1-x^2)^{m/2}}{2^\ell \ell!} \frac{d^{\ell+m}}{dx^{\ell+m}} (x^2 - 1)^\ell$$

are associated Legendre functions,

and $\ell \geq 0$, $|m| \leq \ell$ are integers.



Multipole expansion

The functions $Y_\ell^m(\theta, \phi)$ form a complete orthonormal basis on the sphere:

$$\int_{-1}^1 d \cos \theta \int_0^{2\pi} d\phi Y_\ell^m(\theta, \phi) Y_{\ell'}^{m'}(\theta, \phi) = \delta_\ell^{\ell'} \delta_m^{m'}.$$

Thus any smooth function $f(\theta, \phi)$ can be represented by an infinite series

$$f = \sum_{\ell=0}^{\infty} \sum_{m=-\ell}^{\ell} f_{\ell m} Y_\ell^m(\theta, \phi),$$

or approximated with any desired accuracy by a finite series (up to ℓ_{\max}).

The coefficients of expansion are given by

$$f_{\ell m} = \int_{-1}^1 d \cos \theta \int_0^{2\pi} d\phi f(\theta, \phi) Y_\ell^m(\theta, \phi).$$

Analogously to the Fourier series, the set of terms at a fixed ℓ describes the variation of the function on angular scales $\sim \pi/\ell$,

and is rotationally invariant: $\sum_{m=-\ell}^{\ell} f_{\ell m}^2$ is independent of the basis orientation.

Multipole expansion of the potential

Now we can solve the Laplace equation $\nabla^2 \Phi = 0$ by separation of variables:

assume $\Phi(r, \theta, \phi) = F(r) Y_\ell^m(\theta, \phi)$, then

$$\nabla^2 \Phi = 0 = \frac{1}{r^2} \frac{d}{dr} \left(r^2 \frac{dF}{dr} \right) Y_\ell^m - \frac{\ell(\ell+1)}{r^2} F Y_\ell^m.$$

A power-law solution for the radial part is

$F^-(r) = r^\ell$ (at small radii) or $F^+(r) = r^{-\ell-1}$ (at large radii).

By joining the two solutions at a radius s using Gauss's theorem,

$\frac{\partial \Phi_+}{\partial r} \Big|_{r=s} - \frac{\partial \Phi_-}{\partial r} \Big|_{r=s} = 4\pi G \Sigma$, we get the potential $\Phi_{\ell m}$ of a thin shell with surface density $\Sigma(\theta, \phi) = \Sigma_{\ell m} Y_\ell^m(\theta, \phi)$:

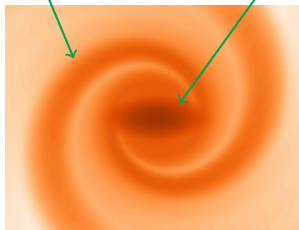
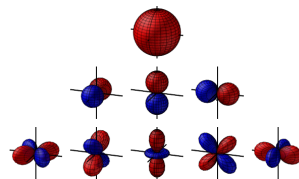
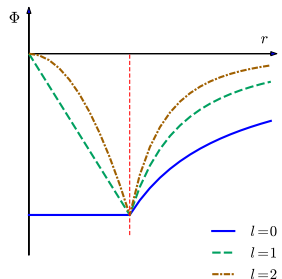
$$\Phi_{\ell m}^- = -\frac{4\pi G s \Sigma_{\ell m}}{2\ell+1} \left(\frac{r}{s}\right)^\ell Y_\ell^m(\theta, \phi), \quad \Phi_{\ell m}^+ = -\frac{4\pi G s \Sigma_{\ell m}}{2\ell+1} \left(\frac{r}{s}\right)^{-\ell-1} Y_\ell^m(\theta, \phi).$$

For a general density profile represented by spherical-harmonic coefficients $\rho_{\ell m}(r)$,

$$\Phi = -4\pi G \sum_{\ell, m} \frac{Y_\ell^m(\theta, \phi)}{2\ell+1} \left[\underset{\text{interior shells}}{r^{-\ell-1} \int_0^r ds s^{\ell+2} \rho_{\ell m}(s)} + \underset{\text{exterior shells}}{r^\ell \int_r^\infty ds s^{1-\ell} \rho_{\ell m}(s)} \right].$$

Properties of multipole expansion

- ▶ The potential of a shell fades more quickly as one moves away in radius for higher-degree harmonics \Rightarrow at large radii, the potential of any finite-mass model is close to a monopole.
- ▶ $\ell = 1$ terms describe the left/right (up/down, etc.) asymmetry and may be cancelled at any given radius by shifting the origin; however, it may not be possible to cancel them *everywhere* if the density profile is intrinsically lopsided.
- ▶ Triaxial systems aligned with the principal axes contain only terms with even ℓ and nonnegative even m ; axisymmetric systems – only $m = 0$.
- ▶ $\ell = 2, m = 0$ term describes the flattening in the z direction (in oblate systems, $\rho_{20} < 0$ and $\Phi_{20} > 0$).
- ▶ $\ell = 2, m = 2$ term measures the y/x axis ratio ($\rho_{22} > 0$ if x is the longer axis).
- ▶ Mirror-symmetric features such as spirals need both $m = 2$ (cosine) and $m = -2$ (sine) terms.



Poisson equation in cylindrical coordinates

Laplacian in cylindrical coordinates R, ϕ, z :

$$\nabla^2 \Phi = \frac{1}{R} \frac{\partial}{\partial R} \left(R \frac{\partial \Phi}{\partial R} \right) + \frac{1}{R^2} \frac{\partial^2 \Phi}{\partial \phi^2} + \frac{\partial^2 \Phi}{\partial z^2}.$$

Again use separation of variables: assume $\Phi(R, z, \phi) = F(R) G(\phi) H(z)$ and seek a solution to $\nabla^2 \Phi = 0$ everywhere in half-space bounded by $z = 0$ (same strategy as in the spherical case, replacing shells by planes).

$$\frac{1}{R F(R)} \frac{\partial}{\partial R} \left(R \frac{dF}{dR} \right) + \frac{1}{R^2 G(\phi)} \frac{d^2 G}{d\phi^2} = -\frac{1}{H(z)} \frac{d^2 H}{dz^2} = -k^2.$$

The solution for $H(z)$ is simple: $H(z) = \exp(\pm kz)$; we want it to decay both at $z \rightarrow +\infty$ and $z \rightarrow -\infty$ and have a break at $z = 0$, so $H(z) = \exp(-k|z|)$.

Multiplying the remaining expression by R^2 , we again separate R and ϕ :

$$\frac{R}{F(R)} \frac{\partial}{\partial R} \left(R \frac{dF}{dR} \right) + k^2 R^2 = -\frac{1}{G(\phi)} \frac{d^2 G}{d\phi^2} = m^2.$$

Thus the solutions for $G(\phi)$ are $\cos m\phi$, $\sin m\phi$.

Poisson equation in cylindrical coordinates

We are left with a more complex equation for $F(R)$:

$$R \frac{\partial}{\partial R} \left(R \frac{dF}{dR} \right) + (k^2 R^2 - m^2) F(R) = 0.$$

The solutions are Bessel functions $J_m(kR)$, $Y_m(kR)$ (the latter are singular at origin and hence not used).

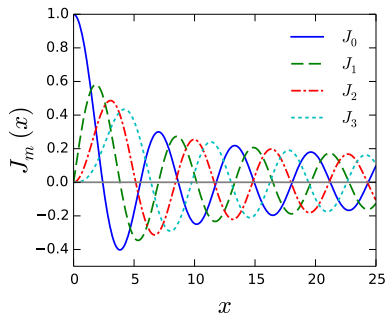
$J_m(x)$ resemble sine functions multiplied by $1/\sqrt{x}$, and many of their properties are analogous to those of trigonometric functions.

In particular, they satisfy the following orthogonality relation:

$$\int_0^\infty dR R J_m(kR) J_m(k'R) = \frac{\delta(k - k')}{k}.$$

The Hankel transform (a.k.a. Fourier–Bessel transform) is a direct analogue of the Fourier transform in cylindrical coordinates:

$$\widehat{F}_m(k) = \int_0^\infty dR R J_m(kR) F(R) \quad \Longleftrightarrow \quad F(R) = \int_0^\infty dk k J_m(kR) \widehat{F}_m(k).$$



Poisson equation in cylindrical coordinates

A single solution of the Laplace equation outside the $z = 0$ plane is

$$\Phi_{km}(R, \phi, z) = J_m(kR) \operatorname{trig} m\phi \exp(-k|z|), \quad \operatorname{trig} m\phi \equiv \begin{cases} \cos m\phi & \text{if } m \geq 0, \\ \sin m\phi & \text{if } m < 0. \end{cases}$$

Using Gauss's theorem, we find that this potential is generated by the following surface density in the $z = 0$ plane:

$$\Sigma_{km}(R, \phi) = -\frac{k}{2\pi G} J_m(kR) \operatorname{trig} m\phi.$$

So the solution for an arbitrary surface density $\Sigma(R, \phi)$ is obtained by these steps:

1. Perform Fourier transform in ϕ to get $\Sigma_m(R) = \frac{1}{2\pi} \int_0^{2\pi} d\phi \operatorname{trig} m\phi \Sigma(R, \phi)$,
2. Perform Hankel transform in R to get $\widehat{\Sigma}_m(k) = \int_0^\infty dR R J_m(kR) \Sigma_m(R)$.
3. Corresponding term in the potential: $\widehat{\Phi}_m(k, z) = -\frac{2\pi G}{k} \widehat{\Sigma}_m(k) \exp(-k|z|)$.
4. The entire potential is given by the inverse Hankel and Fourier transforms:
$$\Phi_m(R, z) = \int_0^\infty dk k J_m(kR) \widehat{\Phi}_m(k, z),$$
$$\Phi(R, \phi, z) = \sum_{m=-\infty}^\infty \Phi_m(R, z) \operatorname{trig} m\phi.$$

Example: potential of an axisymmetric exponential disc

In simple cases, some of the above steps may be performed analytically.

Consider an infinitely thin disc with $\Sigma(R) = \frac{M}{2\pi a^2} \exp(-R/a)$.

Its azimuthal Fourier transform obviously consists of a single $m = 0$ term, and the subsequent Hankel transform gives [GR 6.623]

$$\widehat{\Sigma}_0(k) = \frac{M}{2\pi a^2} \int_0^\infty dR R J_0(kR) \exp(-R/a) = \frac{M}{2\pi (k^2 a^2 + 1)^{3/2}}.$$

Now the potential is

$$\Phi_0(R, z) = -2\pi G \int_0^\infty dk J_0(kR) \exp(-k|z|) \widehat{\Sigma}_0(k).$$

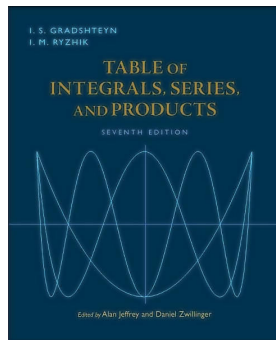
Unfortunately, even Gradshteyn & Ryzhik cannot help with computing this integral analytically, except for $z = 0$:

$$\Phi_0(R, 0) = -\frac{GM}{2a^2} \left[I_0\left(\frac{R}{2a}\right) K_1\left(\frac{R}{2a}\right) - K_0\left(\frac{R}{2a}\right) I_1\left(\frac{R}{2a}\right) \right].$$

Consider now a finite-thickness disc with a separable profile: $\rho(R, z) = \Sigma(R) h(z)$.

By breaking it up into thin planes at each z' , we get $\Phi(R, z) = \int_{-\infty}^\infty dz' \Phi_0(R, z') h(z - z')$ and fortunately, the integral $\int_{-\infty}^\infty dz' h(z - z') \exp(-k|z - z'|)$ can be computed analytically for exponential or isothermal $h(z)$, still leaving a 1d numerical integral in k .

This is not too exciting, and an alternative multipole-based technique is more convenient.



Multipole potential for separable axisymmetric density profiles

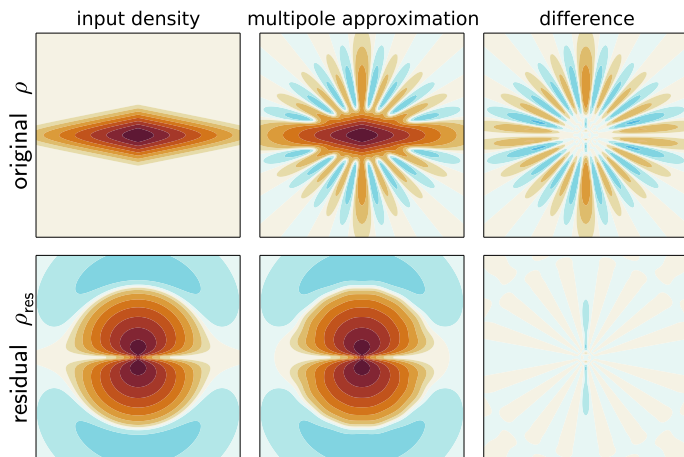
Let $\rho(R, z) = \Sigma(R) h(z)$ and $H(z)$ defined as $H''(z) = h(z)$.

Represent the potential as $\Phi(R, z) = 4\pi G \Sigma(r) H(z) + \Phi_{\text{res}}(R, z)$,
where Φ_{res} is generated by the “residual density”

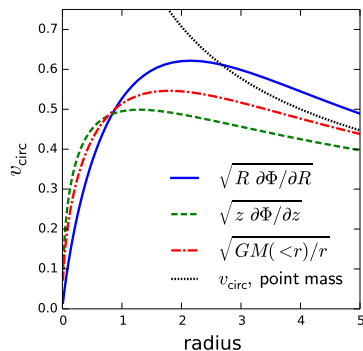
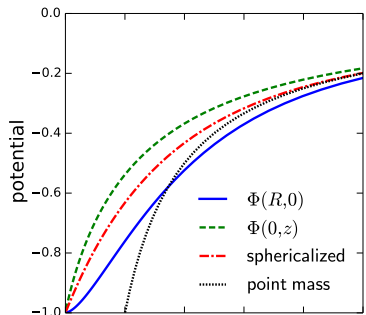
$$\rho_{\text{res}} = \rho(R, z) - \left[\Sigma(R) - \Sigma(r) \right] h(z) - \frac{2}{r} \Sigma'(r) \left[H(z) + z H'(z) \right].$$

This density is not strongly concentrated towards the disc plane and can be efficiently represented by a spherical-harmonic expansion, unlike the original density [Kuijken&Dubinski 1994].

Example for a radially exponential, vertically isothermal disc with $\ell_{\text{max}} = 16$.



Circular-velocity curves in flattened potentials



Define $v_{\text{circ}} \equiv \sqrt{R \frac{\partial\Phi}{\partial R}},$

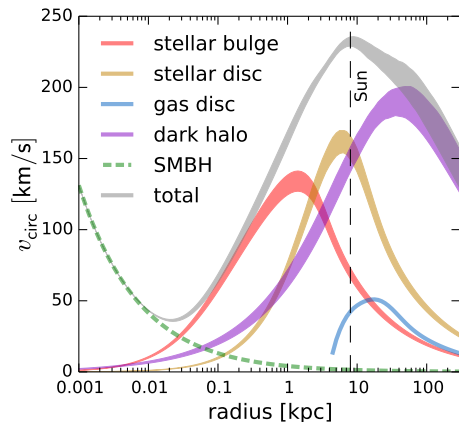
note that $v_{\text{circ}} \neq \sqrt{\frac{G M(< r)}{r}}:$

the potential grows slower along the major axis, and v_{circ} eventually reaches higher values than in a spherical system with the same mass profile.

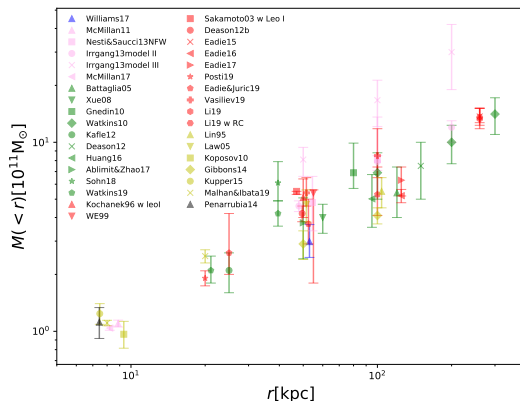
The deviation between v_{circ} and $\sqrt{G M(< r)/r}$ is largest when the density is very flattened, and gradually decreases for thicker discs (the illustration shows an infinitely thin exponential disc with $a = 1$).

Potential of the Milky Way

- ▶ Circular velocity peaks around the Solar radius (8.2 kpc) at $\sim 235 \pm 5$ km/s
- ▶ Stars and dark halo have roughly equal contribution at this radius
- ▶ Mass profile at large radii ($\gtrsim 20$ kpc) is still rather uncertain
- ▶ Total (“virial”) mass within 250–300 kpc is likely $\sim (0.8 - 1.5) \times 10^{12} M_{\odot}$



[McMillan 2017] – pre-Gaia



[Wang+ 2020]

Summary

- ▶ Useful math concepts: confocal ellipsoids, Fourier, Hankel and spherical-harmonic transforms.
- ▶ Equipotential surfaces are rounder than equidensity surfaces.
- ▶ Potential of spherical systems is easy to compute (1d integration).
- ▶ Non-spherical systems generally require 3d integration (with some exceptions, e.g., in ellipsoidally-stratified density profiles);
- ▶ Multipole expansion is often the most efficient way of [approximately] computing the potential, but in the original form it is inaccurate for disk systems.
- ▶ In practice, the solution of the Poisson equation is a solved problem: there exist efficient codes for computing the potential numerically for an arbitrary density profile.